MICROTUBULES IN THE SPERMATIDS OF THE DOMESTIC FOWL

J. RICHARD McINTOSH and KEITH R. PORTER

From the Biological Laboratories, Harvard University, Cambridge, Massachusetts 02138

ABSTRACT

Spermiogenesis in chicken has been examined in order to see whether the radical changes observed in cell shape can be related to the presence of cytoplasmic microtubules. A highly ordered array of tubules has been found which surrounds the nucleus as it elongates from a sphere to a slender cylinder. The structure of the array has been determined by following the tubules through 12–14 adjacent serial sections, and it is a left-handed double helix. Faint cross-bridges connect consecutive turns of the two helices. After the change in nuclear shape is complete, the helical system of microtubules disappears and is replaced by a set of almost straight tubules which run parallel to the long axis of the nucleus. These tubules remain while the spermatid nucleus condenses isotropically to its final size. We suggest that the helix is the agent which effects nuclear elongation and that the subsequent system of paraxial tubules determines the curvature of the final sperm head. Evidence for these suggestions is found in the form of spermatids which have failed to develop properly. In an appendix we consider the kinematics of single and multiple helix systems and discuss the revelance of these models to the morphogenesis of chicken spermatids.

INTRODUCTION

The frequent discovery of microtubular elements in the cytoplasm of asymmetric cells has suggested the hypothesis that microtubules are of general importance in the development and maintenance of biological anisometry (3, 15, 21). One class of asymmetric cell to which the hypothesis should apply is the sperm cell, for the unusual shapes of many mature sperm heads attest to radical transformations of the originally spherical spermatocytes (16). Spermiogenesis in chicken provides an example in which the nucleus changes from a sphere into a long, slender cylinder, tapered at one end and bent into a gentle curve throughout its length. Experience with other asymmetric cells led us to expect to find a system of microtubules associated with the development of this anisometry.

A careful description of spermiogenesis in chicken has been made with the light microscope by Zlotnik (22); Nagano (14), using the electron microscope, has presented a detailed account of some aspects of sperm development as seen in specimens fixed with cold osmium tetroxide or acrolein. The formation of the acrosome and development of the tail structure are covered in these papers, and Nagano has described a manchette of tubular elements which appears after the nucleus is fully elongated. Neither of these papers discusses the labile microtubules which are too small to be resolved in the light microscope and which require special methods of fixation to be seen with the electron microscope. The present paper is an account of chicken spermatid development as seen in the electron microscope after glutaraldehyde fixation, a method known to preserve microtubules in diverse types of cells (1).

METHODS

Adult roosters were killed by dislocation of cervical vertebrae and their testes were immediately removed.

The tissue was cut into blocks of 3 mm in 3% glutaraldehyde (19) buffered to pH 7.5 with 0.1 M sodium cacodylate. After fixation for ½ hr at room temperature, the partially fixed blocks could be cut into pieces small enough to insure good fixation and embedding. A total fixation time of 2 hr was found to be sufficient. The tissue was rinsed in buffer for 2 hr, postfixed at room temperature in 1% OsO_4 buffered with 0.1 M sodium phosphate at pH 7.0 for 1½ hr, and embedded in Epon according to the methods of Luft (11). Sections were cut on a Huxley or a Porter-Blum microtome, stained with uranyl acetate and Reynolds' lead citrate (17), and examined on a Siemens-Elmiskop I. When high resolution microscopy was planned, the tissue was rinsed in water for ½ hr after osmium fixation and then stained in 1% aqueous uranyl acetate at room temperature for ½ hr (C. Franzini-Armstrong. Personal communication). The rest of the procedure was the same.

For serial sections LKB slot grids were used, coated with a gray film of Formvar. Ribbons of 15 sections were picked up on the coated grids from beneath the surface of the water in the boat, stained as usual, and then given a thin coating of carbon.

When measurements were made with the electron microscope, a meter indicating the current in the intermediate lens was calibrated with pictures taken of a replica grating ruled at 33,000 lines per inch. Distances were measured on the plates with a Nikon Shadowgraph model 6C. The standard deviation of measurements of a given structure in different preparations was found to be about 8% of the mean, so the measurements are thought to be reliable to approximately 10%.

OBSERVATIONS

The magnitude of the transformation which occurs during spermiogenesis may be seen by comparing the spermatocytes with the mature spermatozoa. The sizes given here are approximate. At the onset of the transformation, the spermatocytes are roughly spherical with a cellular diameter of 10 μ and a nuclear diameter of 6 μ. In the mature sperm the nucleus, which almost fills the head, is 11 μ long and 0.5 μ in diameter. It is bent to a radius of curvature of 7 μ throughout its length, but the curve is not necessarily planar and helical heads are frequently seen. Therefore, during spermiogenesis the nucleus decreases in volume from 110 μ^3 to 2 μ^3, changes in axial ratio from 1:1 to 22:1, and acquires a defined curvature.

These radical changes in shape and volume come after a series of cytological developments. First, the Sertoli cells send out long processes which completely engulf the spermatocytes (22). The Golgi apparatus then starts the proliferation of membrane-bound vesicles which, with their contents, form the acrosome (2, 22), and one of the centrioles comes to serve as the basal body for the developing flagellum (14). A few scattered microtubules can be seen at this time (Fig. 1). The acrosome and the basal body take up positions at opposite ends of the nucleus and the nuclear material changes in texture. This transformation of the nucleus is accompanied by a decrease in the nuclear volume from about 110 μ^3 to about 25 μ^3 without any substantial change in its spherical shape.

As the nucleus becomes smaller, more microtubules appear and are seen to run in bands around the nucleus (Figs. 2 and 3). The bands show a radius of curvature of about 1½ μ. They lie in planes approximately perpendicular to a line drawn from the acrosome to the basal body, and, as the nuclear material becomes more compact, the tubules form into an ordered array. During this stage, the nucleus loses its spherical form and becomes a prolate ellipsoid whose axial ratio increases as spermiogenesis proceeds.

The bands of tubules are observed as long as the axial ratio of the nucleus is changing, and in the final stages of nuclear elongation there is an exceptionally regular system of microtubules running around the now almost cylindrical nucleus (Figs. 4 and 5). When the plane of section is perpendicular to the axis of the spermatid, the individual loops are seen to have a constant radius of curvature (Fig. 4, insert); when the section contains the axis, the regularity of the spacing between the tubules is evident (Fig. 5, inserts).

No single electron microscope picture of the array can disclose the exact structure of this orderly system of tubules, for any one micrograph could be interpreted either as a set of closed rings stacked on top of one another or as a set of one or more helices with the same sense, i.e., a right- or left-handed screw. For example, in Fig. 4 the tubules appear to form closed loops, but since the section includes at least two layers of tubules, the image could equally well be the result of the overlapping of consecutive turns of a helix.

We have been able to decide between these alternatives by cutting serial sections parallel to the long axis of the spermatid. 12–14 serial sections showing silver as an interference color provided enough depth to allow us to follow one tubule all the way around the nucleus.

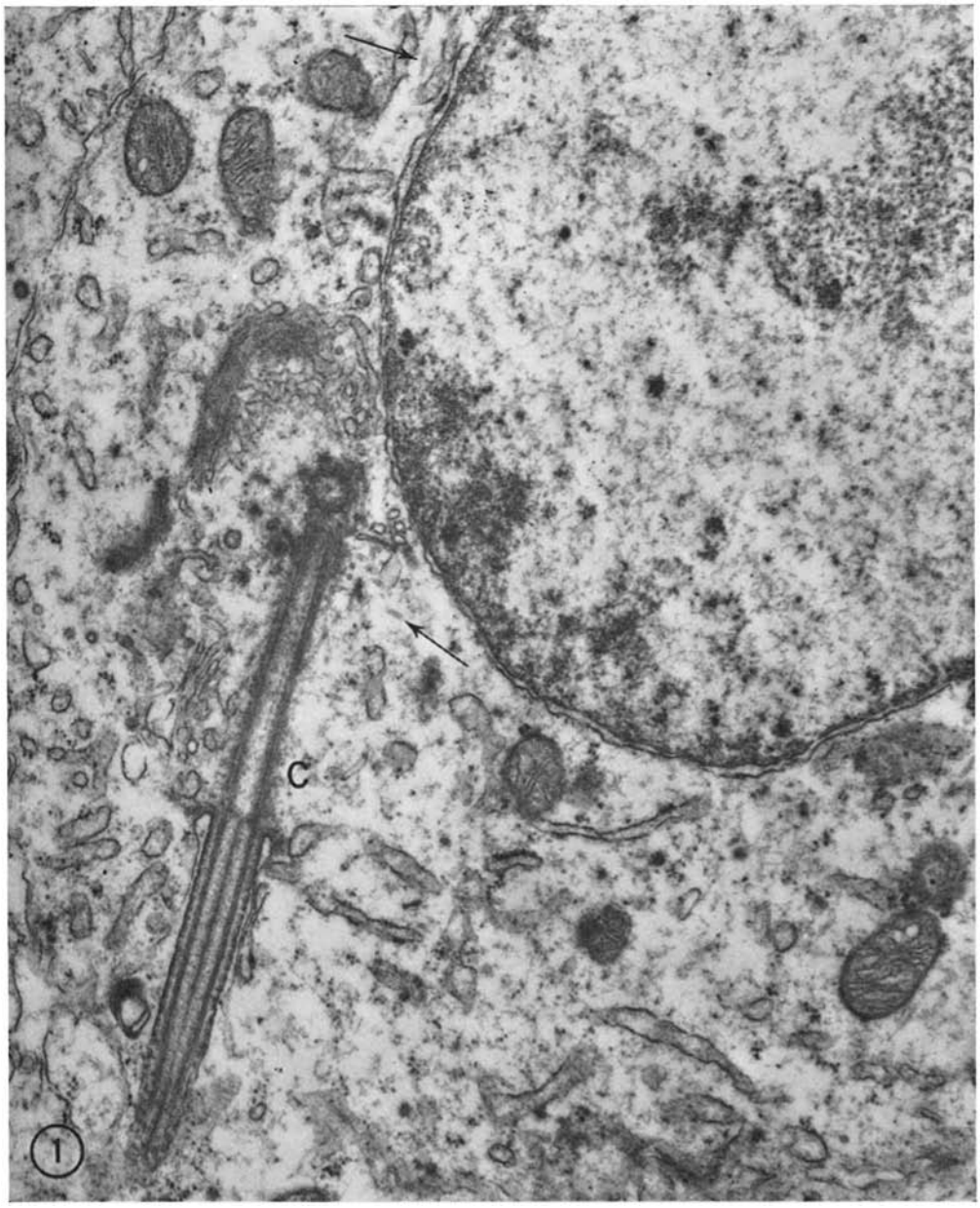

FIGURE 1 An early spermatid before nuclear elongation, with a tail developing from the centriole (*C*). A few microtubules are seen near the centriole and the nuclear envelope (arrows). × 25,000.

Tracing any given tubule from picture to picture was difficult, for there are no special features which distinguish one tubule from another. We therefore identified specific tubules by their position with respect to structural features which could be followed clearly from one picture to the next: an acute bend in a membrane running perpendicular to the plane of section, imperfections in the tubule array, or points of symmetry in an organelle such as a mitochondrion. Figs. 6 *a* and *b* is a pair of adjacent sections with eight identifiable structures marked on each picture. Distances can be meas-

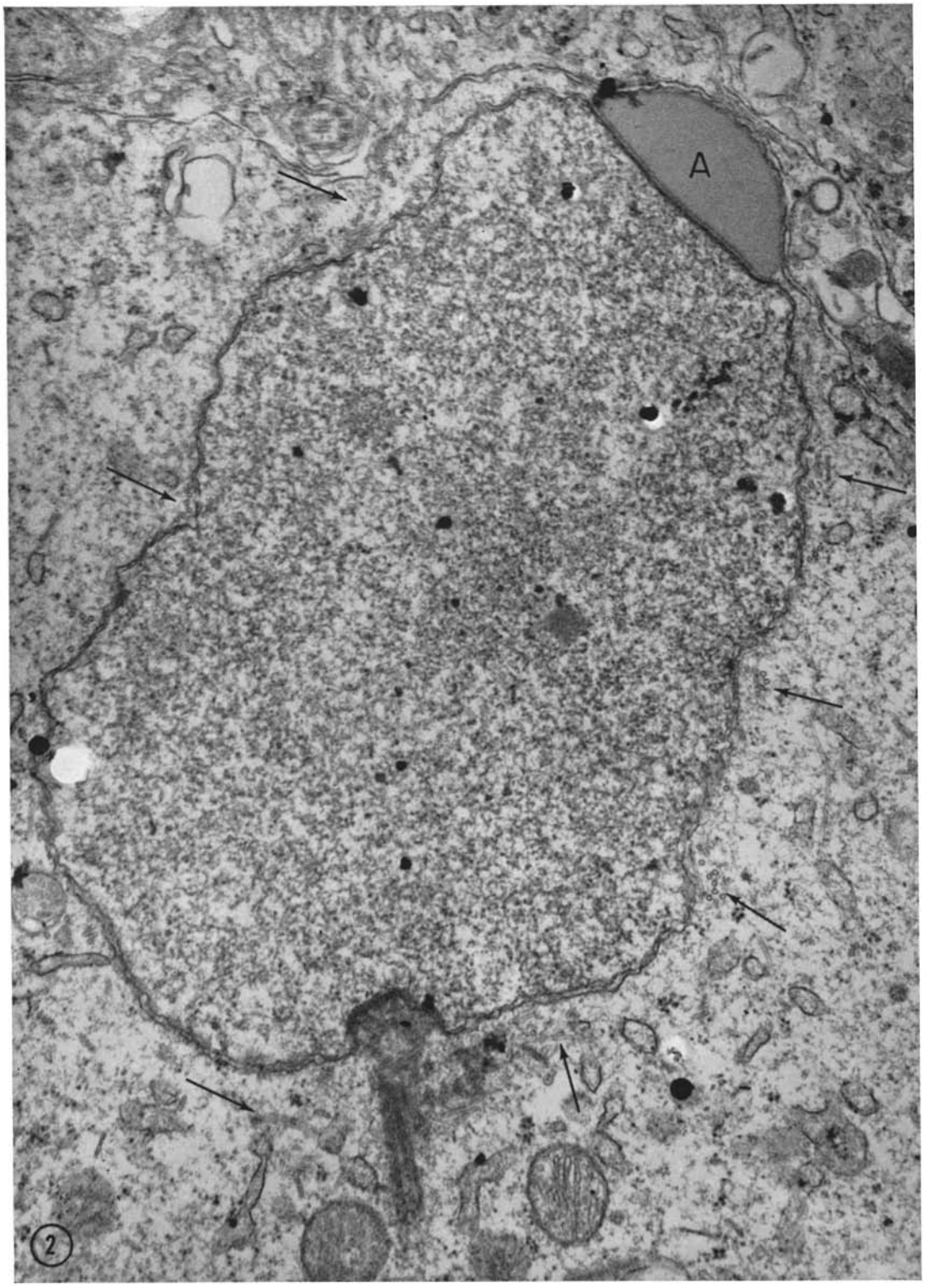

FIGURE 2 The acrosomal cap (*A*) is attached to the nuclear envelope, the chromatin has changed in texture, and nuclear elongation has just begun. Tubules are now present in the region around the basal body of the tail, and a few bands of tubules already encircle the nucleus (arrows). The radius of curvature of the tubules around the nucleus is 1¼ μ. × 40,000.

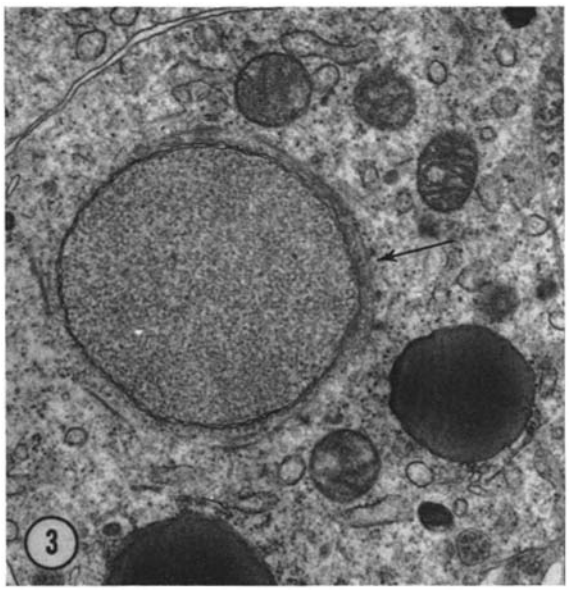

FIGURE 3 A cross-section of the developing nucleus showing the bands of tubules just outside the nuclear envelope (arrow). The radius of curvature of the tubules is 1 μ. × 20,000.

ured from these points to any chosen tubule on one micrograph and then can be mapped out on the next section in order to identify the corresponding tubule. It is necessary to remember that structures which are not running perpendicular to the plane of section will have shifted position in a predictable fashion from one section to the next. A full set of 13 plates is not published here for reasons of space, but Figs. 7 *a–m* shows a small region from each plate in a complete serial sequence. Figs. 7 *f* and 7 *g* are subregions of Figs. 6 *a* and 6 *b*, so the relationship between the size of the full plate and of the subregion can be seen. The arrows in Fig. 7 indicate the corresponding tubule in each picture, since there is not sufficient area shown for the reader to establish the sequence for himself in all cases.

The tracing of tubules through serial sections was carried out in two or more regions of nine different spermatids. In almost every case, we found that when a given tubule completed its circuit around the nucleus, it did not return to its original location, but rather had moved two tubules along the length of the nucleus. The simplest interpretation of this observation is clearly that the system of tubules which surrounds the nucleus is a double helix. (A displacement of one step would indicate a single helix; a return of each tubule to its starting point would indicate a stack of rings unconnected to one another.) The sense of the helices has been determined in seven spermatids: it was left-handed in each case.

Only two instances were found in which the tubule did not move two places in one circuit around the nucleus. Both appear to be aberrations from the normal pattern and are interesting examples of the kinds of error which occur at this level of biological order. In one case, the displacements in three successive turns around the nucleus were three, one, and two steps. In this region of the helix, there were two loops of tubule in the same plane, one outside the other, so the mistake is probably related to the extra loop. The second aberrant pattern showed a displacement of four steps in a single circuit, but an obvious dislocation in the lattice at this point probably accounts for the shift. During its next trip around the nucleus, this tubule was displaced the normal two steps.

When the nucleus has reached its maximum length, the helices run from the base of the acrosome to the caudal end of the basal body (Fig. 5), a distance of about 24 μ. The center-to-center spacing of the tubules in the helices is 300 A $\pm$ 10%. Since there are two helices present, the pitch of each helix is 600 A. The diameter of the helices in their final form is about 1 μ, so the angle of

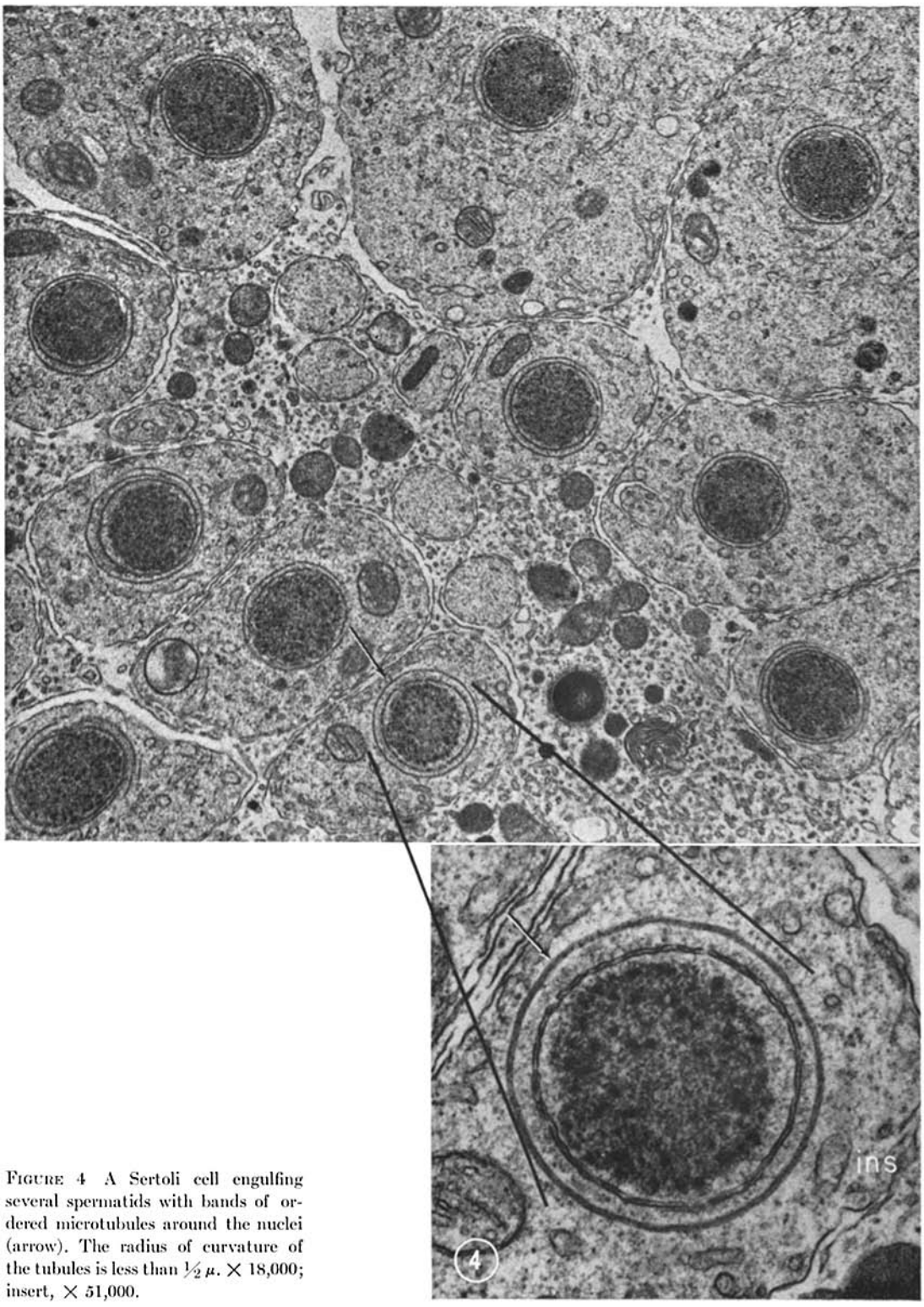

FIGURE 4 A Sertoli cell engulfing several spermatids with bands of ordered microtubules around the nuclei (arrow). The radius of curvature of the tubules is less than ½ μ. × 18,000; insert, × 51,000.

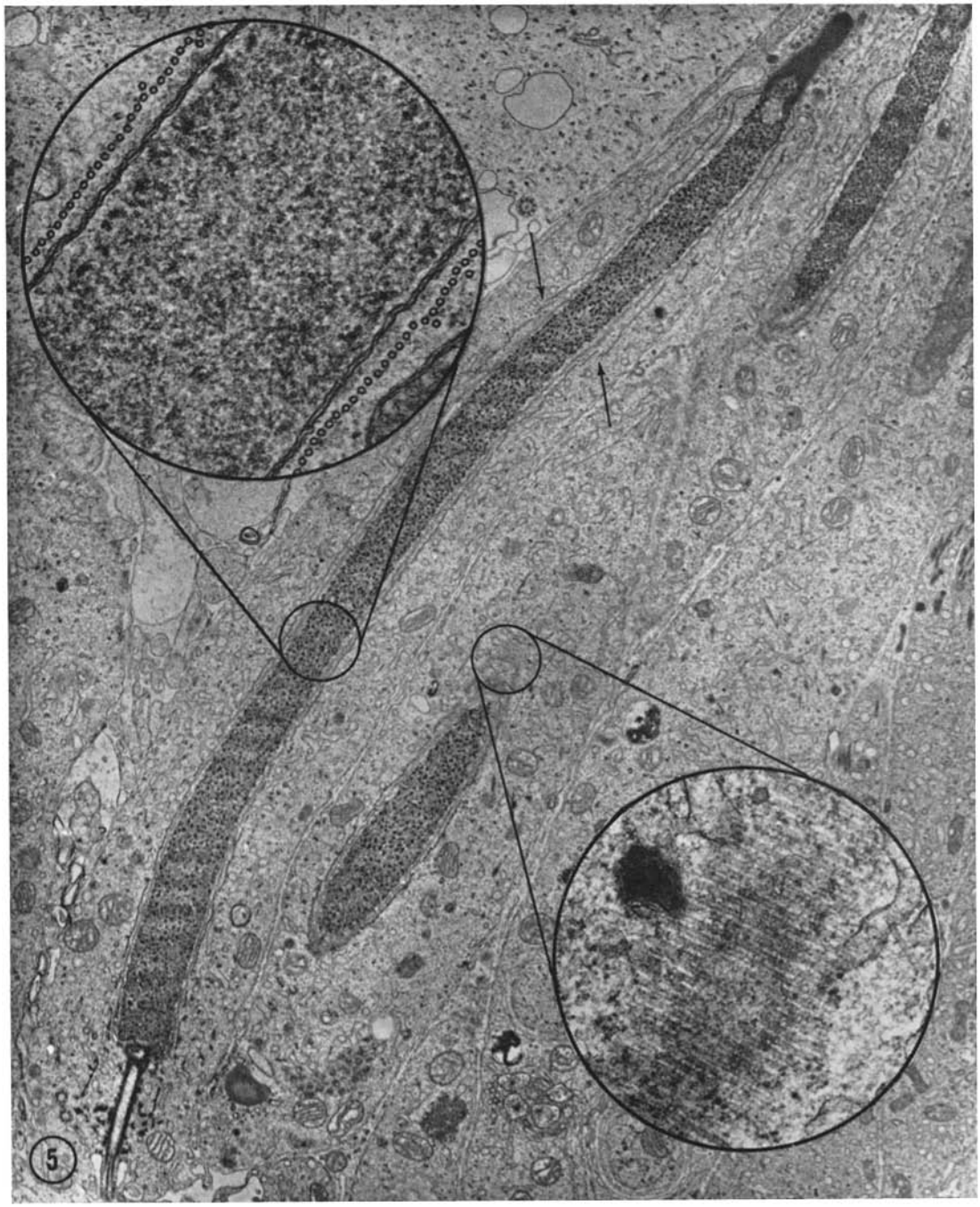

FIGURE 5 An axial section of the spermatid after complete nuclear elongation showing the extent of the tubule array. Note that the array is interrupted (arrows). × 9,400. The inserts are taken from another plate of higher instrument magnification; they show comparable areas from a different spermatid. × 56,000.

inclination of each helix is approximately 1.1°. Each spermatid at this stage of development, therefore, contains about 2,500 μ of cytoplasmic microtubular material.[1]

The center-to-center spacing of the tubules occasionally deviates widely from the mean value of 300 A. These gaps generally occur in pairs on either side of the nucleus and seem to represent breaks in the helices (Fig. 5, arrows); all helices appear to be divided into segments by such gaps. The length of the segments is, however, not uniform.

When the center-to-center spacing of the tubules in the helix is regular, the tubules would seem to run around the nucleus without interruption. A helix segment containing uniform center-to-center spacing will frequently extend for 2 μ along the nucleus, suggesting that one tubule can be as long as 100 μ.

The tubules themselves have the same diameter as previously reported cytoplasmic microtubules which have been fixed in glutaraldehyde and embedded in hard plastic (15). They have an outside diameter of 240 A ± 10% and an inner diameter of 110 A ± 10%. The diameter of the tubules is more consistent than the experimental error would indicate. Using a Nikon Shadowgraph, we measured the dimensions of 20 tubules on each of three plates which we had micrographed with care to minimize distortion effects, and, in all cases, the standard deviation of the measurements was approximately 4% of the mean for the plate.

No precise statement can be made about the symmetry of the tubules, for it has not been possible to resolve the subunits clearly in sectioned material. After counting the apparent number of subunits in a large number of tubules and using Markham's (12) method for reinforcement of rotational symmetry, we can say that the structure possesses an axis of rotation which is 13-fold ± 1. This is consistent with the information available for microtubules found in plant cells (10).

The pitch of the helices seems to be as precisely determined as the diameter of the tubules themselves. We calculated the standard deviation of the center-to-center spacing of the tubules in the helical array by taking 20 measurements on each of three plates and found that it was again only 4% of the mean for the plate. The regularity of the periodicity implies that some structure is present which governs the relative position of successive turns of the helices. Pictures of good resolution show a fine connection between the tubules (Fig. 8 *a* and *b* and Fig. 6 *a* and *b*). These bridges may serve to determine the regular spacing of the tubules.

The connections between the tubules are similar to the ones described by Grimstone and Cleveland (5) in the axostyle of several flagellates, but are not so well defined as the bridges seen by Robison (18) in the sperm syncytium of a scale insect. In the previously described systems, the position of the bridges suggests that they are part of a motile mechanism. It is possible that this is also true of the connections seen in the helices of microtubules found in chicken spermatids. When the connections are visible between turns of the helices, they are spaced at intervals of about 600 A along the tubule (Fig. 8 *a*), but, in general, the quality of structural preservation does not permit definite conclusions about periodicity.

When the spermatid nucleus reaches its full length of 22 μ, it is 1 μ in diameter and, therefore, larger in all dimensions than the mature sperm head. The final stages of spermiogenesis involve a

[1] Since the pitch of the helix is small in comparison with the circumference, each turn of the helix contains about $2\pi r = 3.1\ \mu$ of tubule. The total length of cytoplasmic tubule in the spermatid is

$$2 \times \frac{\text{helix extent}}{\text{helix pitch}} \times \text{length per turn} =$$

$$2 \times \frac{240{,}000}{600} \times 3.1\ \mu \approx 2{,}500\ \mu.$$

FIGURE 6 A pair of adjacent serial sections with eight structures marked which can be traced from one picture to the next (stars). Figs. 6 *a* and *b* show almost all the original plates from which Figs. 7 *f* and *g* were taken. A tubule may be chosen on one picture and identified in the next by measuring the relative distances from structures such as those marked. It is necessary to allow for the fact that if the identifying structure is not running perpendicular to the plane of section, it will have moved to a new position which is predictable from its initial orientation. × 58,000.

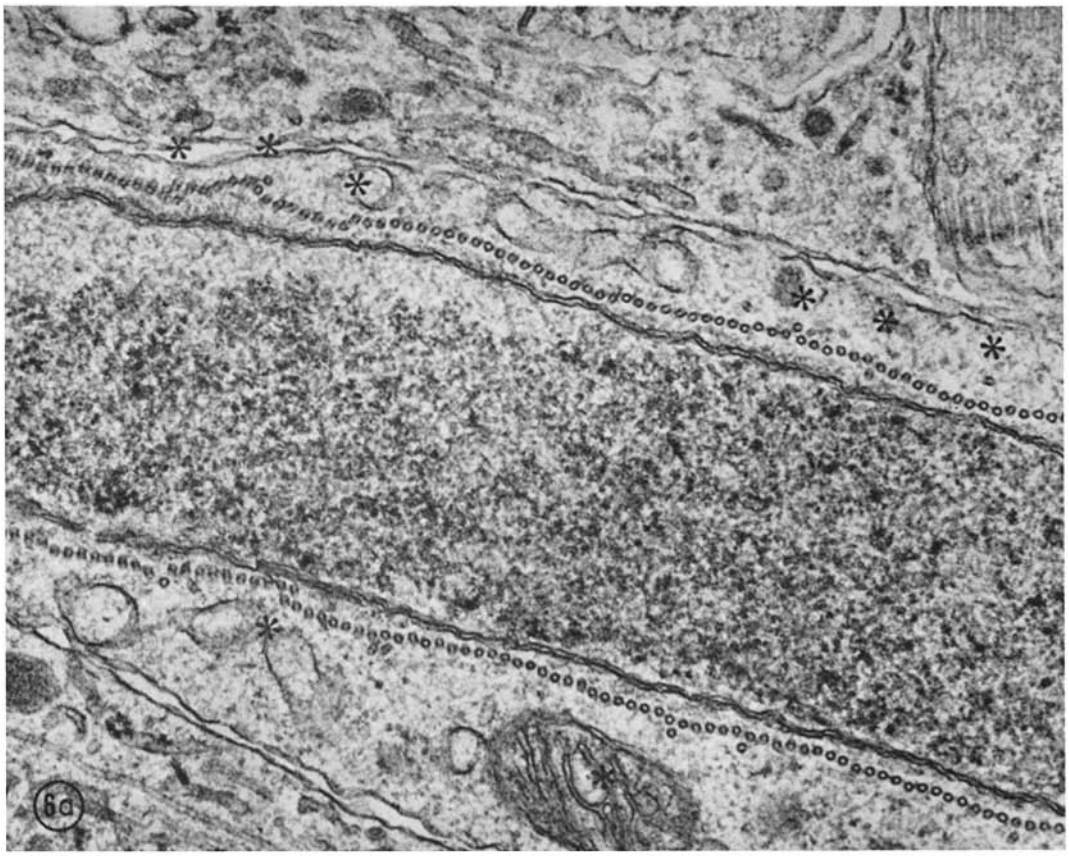

6a

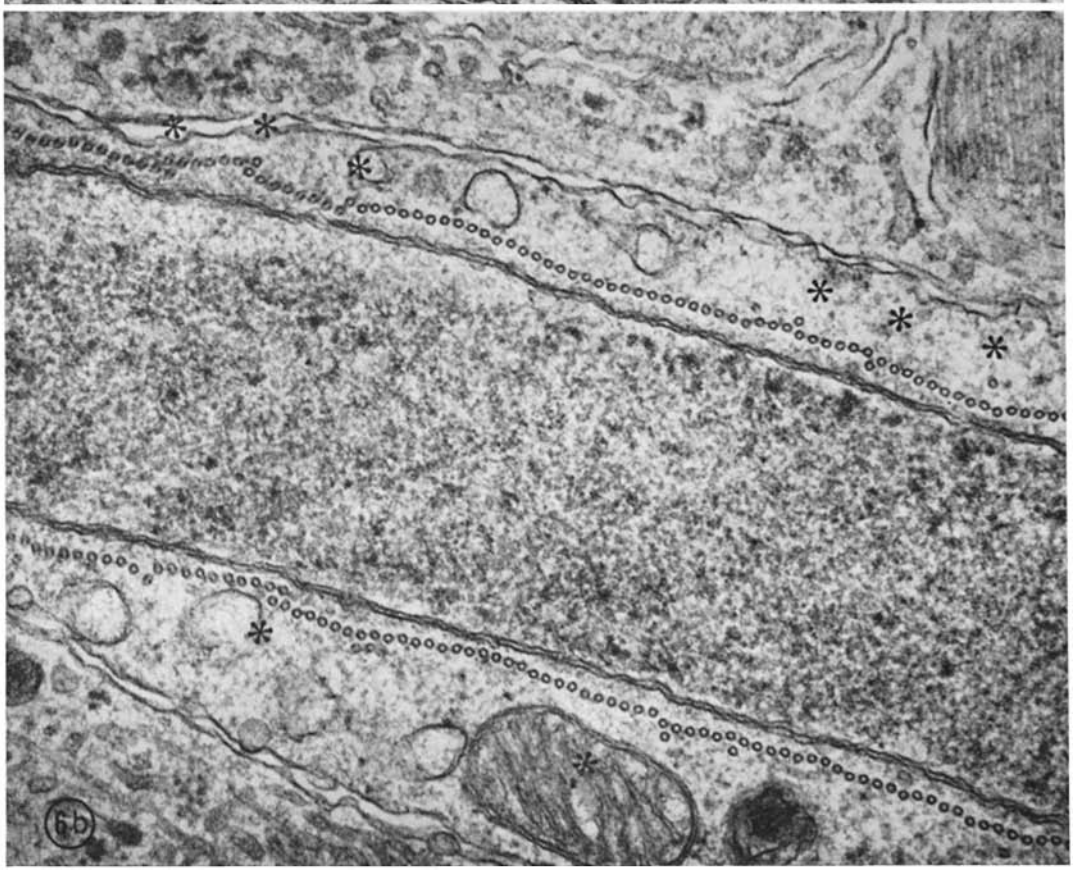

6b

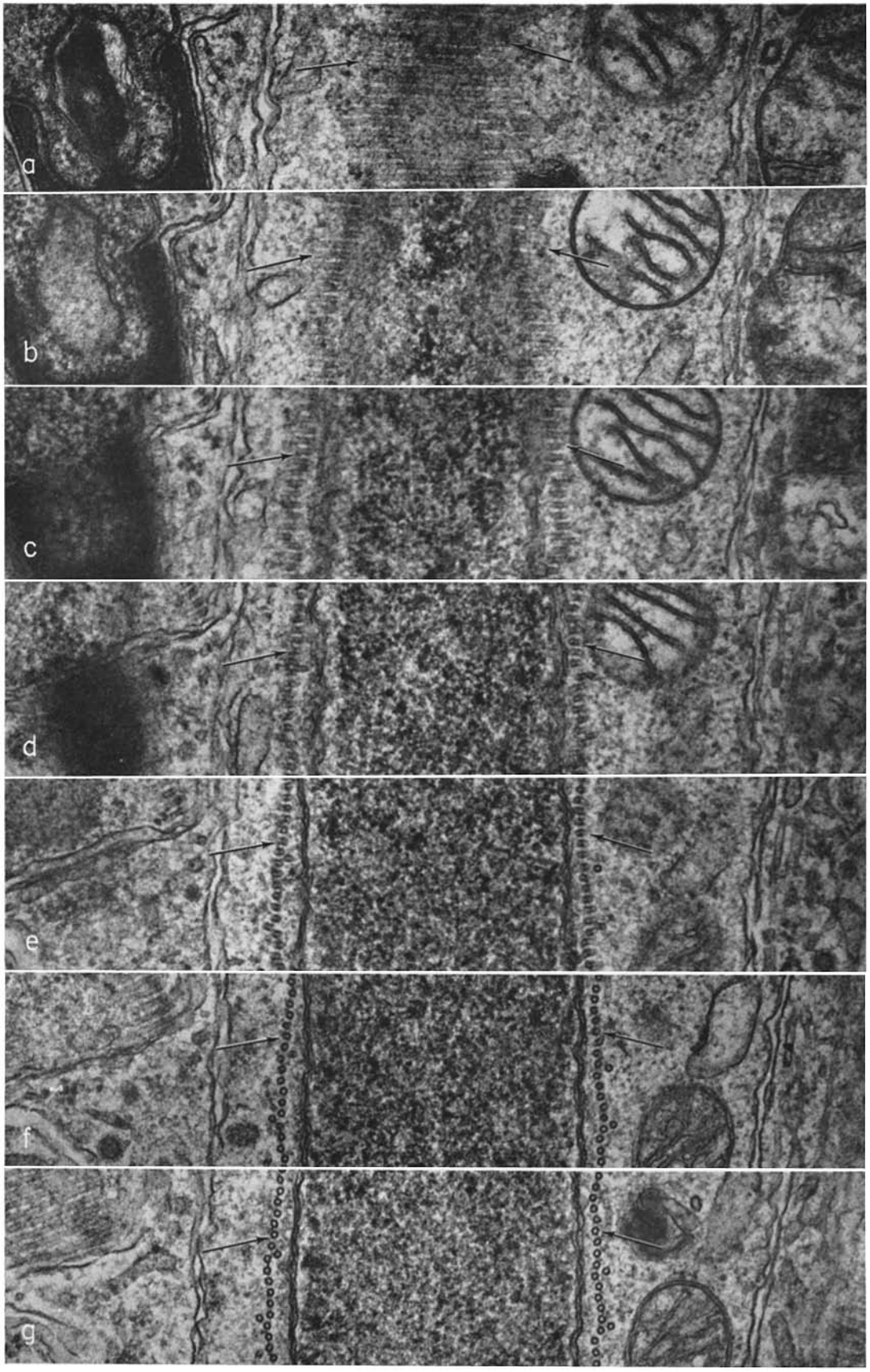

FIGURE 7 a–g (*for legend see opposite page*)

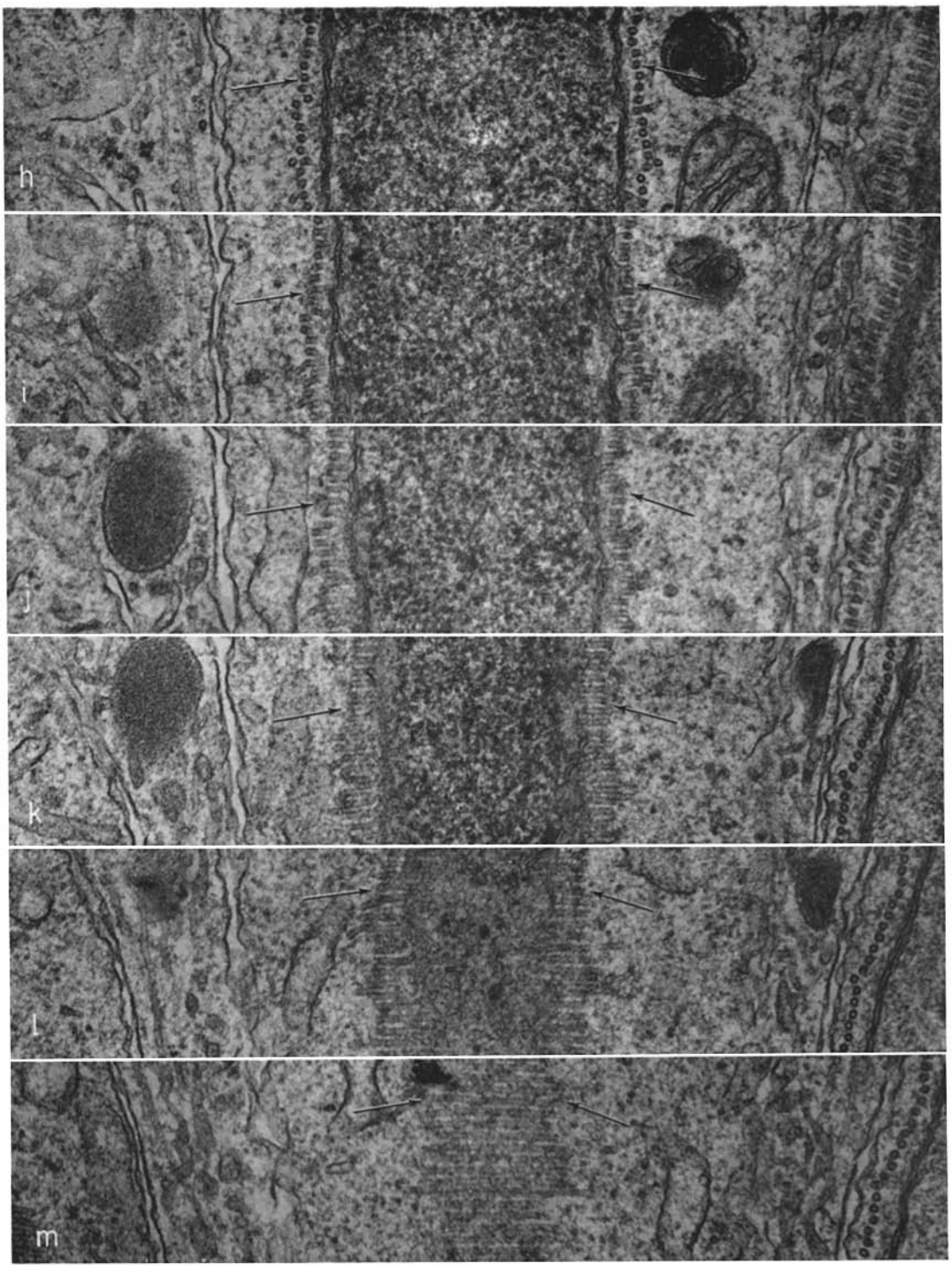

FIGURE 7 h–m

FIGURE 7 *a–m* Cut-outs of small regions on plates of 13 consecutive serial sections approximately 900 A thick. The arrows follow one tubule to the far side of the spermatid and back again. × 58,000.

condensation of the nuclear material into a state which stains with heavy metals to total electron opacity. After nuclear elongation is complete, dense granules about 400 A in diameter appear in the nucleus (Figs. 4 and 5, and Fig. 9), and they coalesce to form the dark-staining material which constitutes the mature sperm head (Fig. 10). Concomitant with this change is a decrease in nuclear volume. The shrinking seems to be isotropic, since the ratio of final size to the size at the stage of maximum length is approximately the same in all directions.

Shortly after the dark-staining granules begin to appear in the nucleus, the system of helically arranged tubules disappears and is replaced by a new array of almost straight tubules lying parallel to the long axis of the spermatid (Fig. 9). Judged by the infrequency with which transition stages are found, the change is rapid in comparison with the remainder of the process. This set of straight tubules has been described by Nagano (14) and corresponds to the manchette seen in the light microscope. The tubules of this array extend from the region of the cytoplasm immediately around the acrosome past the basal body of the flagellum and into the bag of cytoplasm which surrounds the sperm tail. There is no apparent consistency in either the number of tubules or the spacing between them. 30 spermatids contained an average of 200 tubules per sperm with a standard deviation which was 20% of the mean. Their center-to-center spacing was 600 A ± 40%.

The tubules of the manchette display considerable variation in the thickness of their walls. When they first appear, the tubules have an outer diameter of about 240 A, an inner diameter of 110 A, and a rotational symmetry of about 13: they are thus morphologically similar to the tubules of the helix. The same measurements made on tubules surrounding very dense nuclei show that although the inner diameter is about the same and the symmetry is not observably changed, the outer diameter is now between 350 and 400 A. If the staining properties of the nucleus are accepted as an adequate clock to order the events of spermiogenesis, the variation in the tubule wall can be attributed to a gradual thickening as the spermatid matures (Fig. 10 *a–c*). Fig. 10 *d* shows that the thickening of the tubule wall also occurs in the portion of the manchette which surrounds the tail.

We measured the tubules described by Nagano (14), which he fixed with cold osmium tetroxide or cold acrolein, and found them to be similar in size to the thick-walled tubules which we pre-

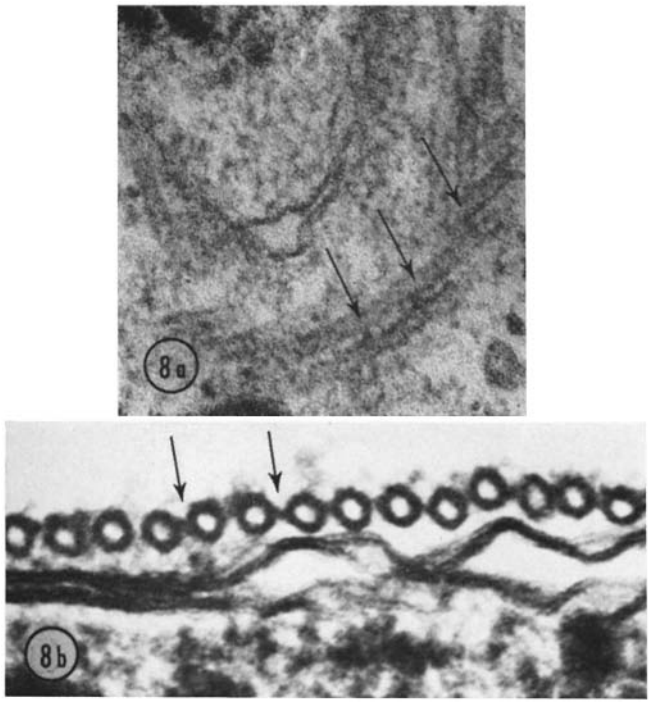

FIGURE 8 Pictures of the helical tubules in longitudinal section (8 *a*, × 135,000) and in cross-section (8 *b*, × 200,000), showing a fine connection between adjacent tubules.

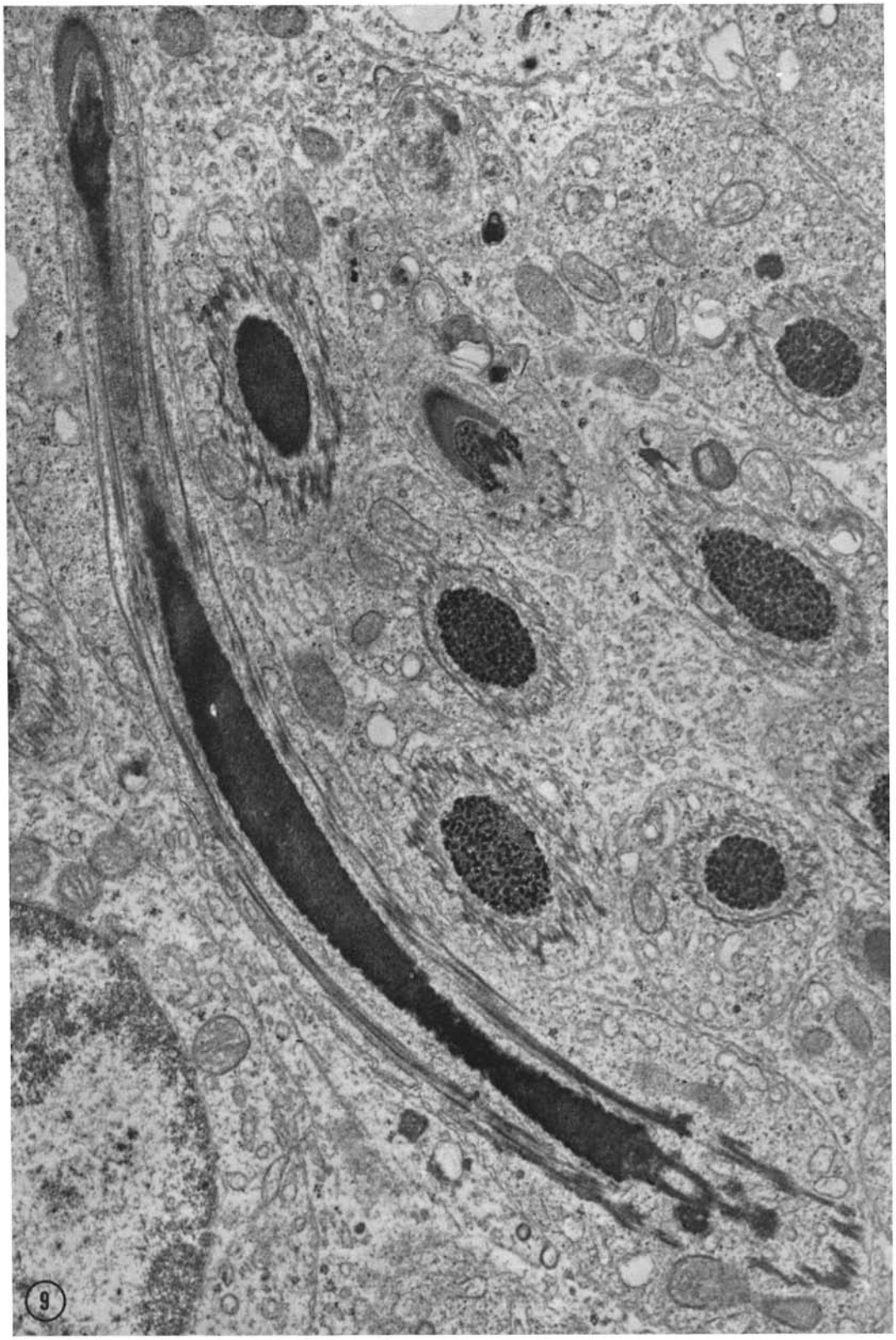

FIGURE 9 After nuclear elongation is complete, the helix disappears and is replaced by a system of tubules which runs parallel to the axis of the nucleus. This is the manchette seen in the light microscope. × 18,000.

served with glutaraldehyde. The thin-walled tubules of the earlier stages must, therefore, be unstable under the methods of fixation which Nagano employed. It is not surprising that glutaraldehyde fixes both kinds of tubules, but we have found that acrolein, when used at room temperature, will preserve the helix and all stages of manchette tubules. Since cold acrolein does not preserve the helix, temperature seems to be a factor in the stability of these tubules. Apparently the thin-walled tubules possess the positive entropy of polymerization described by Inoué (7) for the birefringent elements of the mitotic spindle, by Lauffer et al. (9) for the protein of the tobacco mosaic virus coat, and by Tilney (20) for the tubules in the axopods of the protozoan *Actinosphaerium*.

Before the manchette appears, the axis of the nucleus is nearly straight. Any minor bends which occur do not turn the spermatid systematically one way or the other. After the manchette has developed, however, the nucleus assumes a curve with

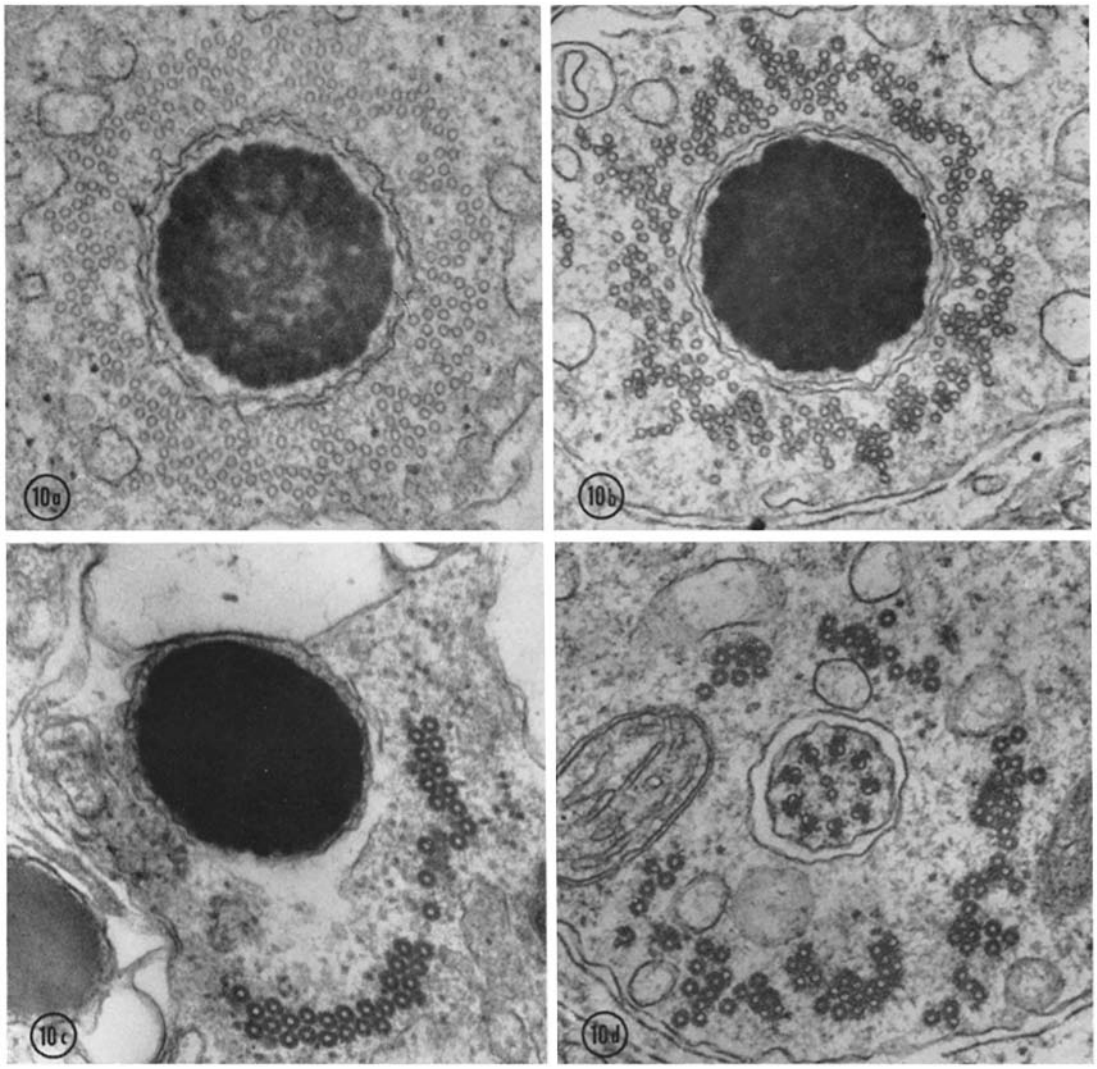

FIGURE 10 *a–c* A group of successively darker nuclei and hence successively later spermatids. The thickness of the tubule wall seems to increase as the spermatid develops. The method of fixation and staining is the same in each case, although the samples do not come from the same preparation. Fig. 10 *d* shows the thickening of the tubule wall in the region of the manchette around the tail. × 54,000.

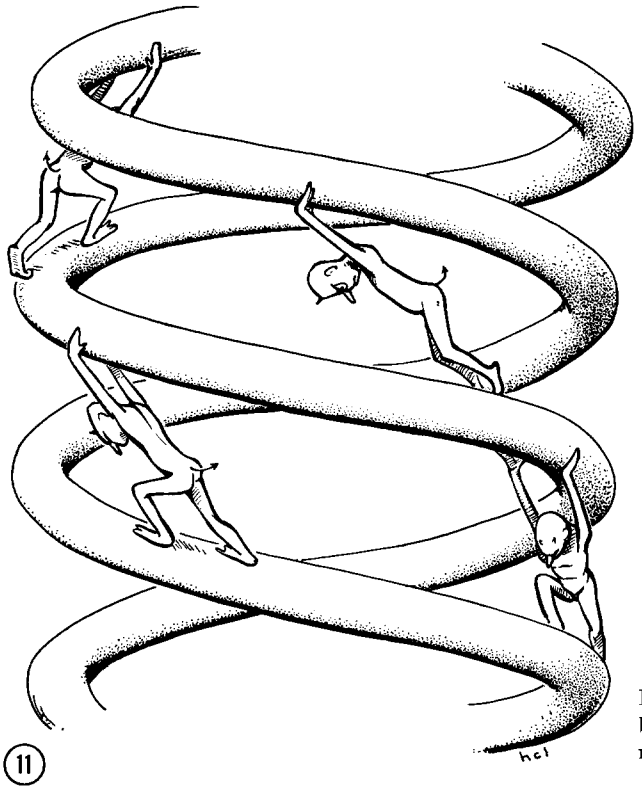

FIGURE 11 A representation of what may be happening to the helix of tubules as the nucleus is elongating.

a radius of 7 μ (Fig. 9). The curve is sometimes planar and sometimes helical, but the curvature is consistent within the accuracy of measurement. This is the shape of the mature sperm head as seen in the light microscope.

The manchette surrounds the nucleus throughout the period in which the granular condensation of the chromatin takes place. When, however, the nuclear material has reached a state indistinguishable from the head of the mature sperm, the number of tubules seen in the manchette is markedly reduced. Thus, in Fig. 10 *b* there are about 250 tubules (i.e., more than the mean number of 200), whereas in Fig. 10 *c* there are only 38. Some of the tubular material apparently dissolves into the ground substance of the cytoplasm, and the few remaining tubules are probably sloughed off with the residual cytoplasm.

DISCUSSION

A. *Function of the Tubule Systems*

The development of two separate tubule systems at distinct stages in the process of spermiogenesis suggests that the arrays have different and well defined functions. We believe that after the initial decrease in nuclear volume, the helix of tubules effects the change in nuclear shape, perhaps by means of the faint cross-bridges seen between adjacent tubules. In muscle cells, it is probable that the cross-bridges act to force the thin filaments past the thick ones. If the tubule cross-bridges acted in an analogous fashion, we should expect to see the pitch of the helices remain constant while the diameter decreased and the over-all length of the helices increased (see Appendix).

We have observed that the intertubule spacing is consistently 300 A during the stages of development in which the helices are well established, and even at the earliest stage of helix formation when only isolated groups of tubule loops are present, the spacing between the tubules within a group is 300 A. The diameter of the helix, however, does not remain constant. In the early stages, the radius of curvature of the loops of tubules is about 2 μ, whereas the final helix radius is less than $\frac{1}{2}$ μ. Further, during nuclear elongation the length of

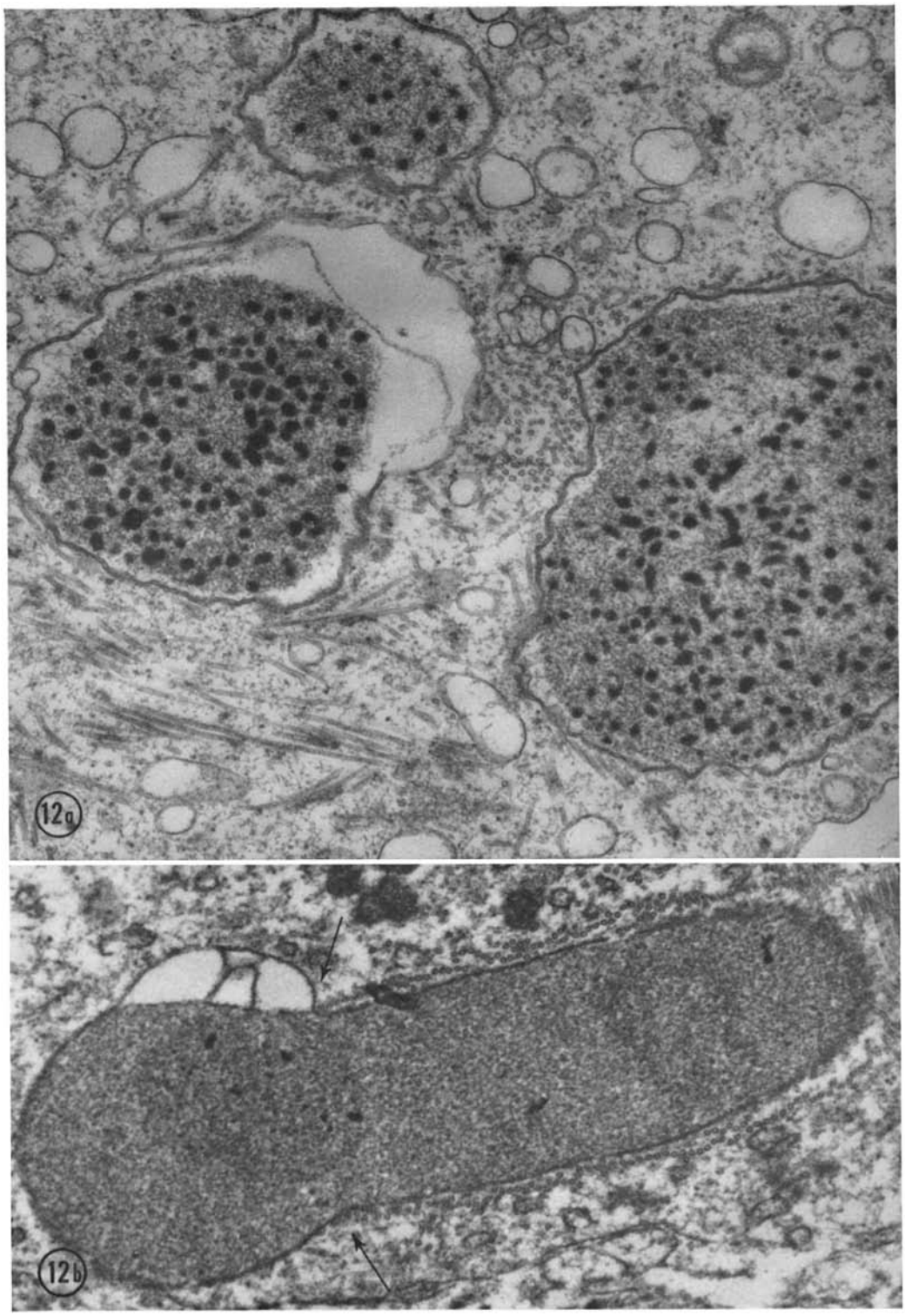

FIGURE 12 Two aberrant spermatid nuclei which show mistakes in the arrangement of the helical tubules. Fig. 12 *a* shows a nucleus whose chromatin is in the stage normally contemporaneous with a fully elongated nucleus. No such elongation is seen, and the many tubules present are in conspicuous disarray. × 35,000. In Fig. 12 *b*, the arrows show the point at which the helix appears to end, and at just that point a bulge occurs in the nucleus. × 38,000.

the helix grows from a few bands of tubules to about 700 turns.

We suggest, therefore, that the cross-bridges are involved in forcing successive turns of the helices to slide over one another. According to this interpretation, the sliding would develop a radial component of force which would constrict the nucleus, reducing its diameter and forcing it into a cylindrical shape. Fig. 11 shows a model of helical sliding in order that the geometry of the situation may be plainly seen: the question of cross-bridge mechanism is put aside by employing a team of modified Maxwellian demons. A more detailed account of the motions and the forces developed in the model is given in the appendix of this paper.

Evidence supporting the suggestion that constriction by the helical array is necessary for nuclear elongation is found in the tubule systems of spermatids which have failed to develop properly. Two classes of aberrant cells have been seen which pertain to the helical tubules. We have found several nuclei which showed the dense granules characteristic of the final condensation stage which occurs after nuclear elongation, but which were several times larger in diameter than normal nuclei at this stage and which were irregular in shape rather than cylindrical (Fig. 12 *a*). Apparently, the mechanism for changing nuclear shape had failed in these spermatids. There were many microtubules present in the malformed cells, but they showed no ordered arrangement such as the helical array of the normal spermatids. A second mistake in spermiogenesis associated with the helix was a case in which a small region of the nucleus had bulged out to 1½ times the normal diameter, although the rest of the nucleus was normal in size and shape (Fig. 12 *b*). The helix of tubules was regular except for the area of the bulge, at which point it was absent. Both these examples of misshapen nuclei corroborate the suggestion that the helix is a determinant of nuclear shape.

We suggest further that the manchette of tubules serves to maintain the long form of the nucleus as the granular condensation of the chromatin occurs. The inherent rigidity of tubular structures (15) would enable the manchette to support the extended and flexible nucleus until it had condensed into a state sufficiently rigid to maintain its shape without external reinforcement.

There are aberrant spermatids whose malformations seem to be related to mistakes in the organization of the manchette. It is not uncommon to find spermatids in which the nucleus has coiled up after elongation (Fig. 13). This image was actually seen often enough by two early investigators using the light microscope for them to propose uncoiling as part of the normal process of spermiogenesis (6, 22). We have found that in such cells the manchette of tubules either was separated from the nucleus and lay in another part of the cell, or was missing altogether. Since the nucleus coils in the absence of the manchette, it is probable that the straight tubules function to maintain the elongated form.

The mature nucleus is not, however, entirely straight, and the manchette may well be involved in the establishment of the defined curvature. If

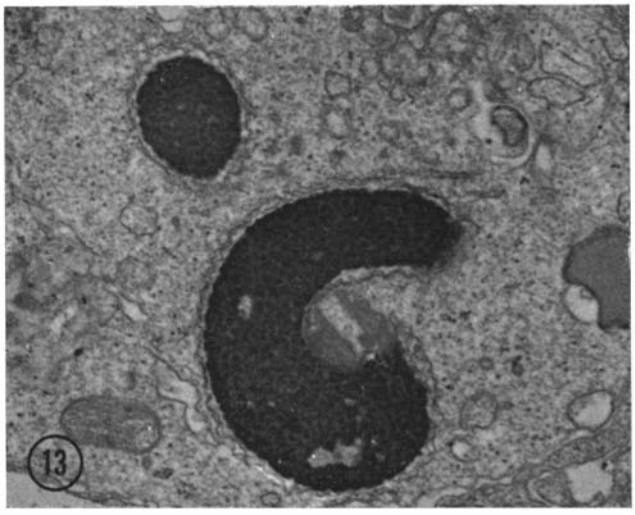

FIGURE 13 An aberrant spermatid nucleus which does not have a manchette. A nucleus with chromatin in this condition would normally be curved in a gentle arc of 7-μ radius. A tight curve such as this is found only in the absence of a manchette. × 25,000.

the tubules of the manchette were naturally straight and if the nucleus tended to coil as it condensed, a static equilibrium would result from the stress imposed by the curving nucleus upon the straight manchette. The fact that the nucleus does coil tightly in the absence of the manchette supports the idea that the normal curvature is the result of the interaction between the nucleus and the system of microtubules.

B. *Relation between the Tubule Systems*

We propose that the major structural component of the microtubules in both of these systems is a protein. Our suggestion is based on an analogy with better studied systems such as the TMV coat (8), the nine-plus-two structure of cilia (4), and hemoglobin from sickle-cell erythrocytes (13). Each of these contains tubular structures which have been shown chemically to consist of protein.

It would be interesting to know whether the structural material of the two types of cytoplasmic tubules found in chick spermatids is the same. We have no experimental evidence on this point at present, but several considerations favor the view that the subunits of the helical tubules are re-used to make up the nearly straight tubules of the manchette. These points are: the morphological similarity of the tubules in the two systems; the fact that in the transition phase one array appears as the other disappears; the difficulty of synthesizing a large amount of macromolecular material at a time when the cytoplasmic volume has been substantially reduced and when the cytoplasm which is left contains few of the free ribosomes generally associated with synthesis; and the improbability that the material needed to make the tubules of the manchette (about 10^7 macromolecules[2]) would be presynthesized and stored in a cell in which the cytoplasmic volume is being reduced by a factor of 8.[3]

If the material of the different tubule systems is the same, clearly the subunits must change their pattern of assembly at the stage of transition from one form of tubule to the other. The thickening of the wall of the second type of tubule may be related to this change in assembly, since the rearrangement of bonding sites might easily expose previously hidden chemical groups which would gradually bind material from the ground substance, thereby changing the staining properties of the wall.

It seems probable that the tubules of both systems exhibit the property of self-assembly characteristic of the folding of polypeptide chains and the polymerization of the TMV coat. According to the self-assembly model, the proper physical conditions would induce the tubules to form as a solid state of the subunits which had been free in solution. Presumably, however, some organizing system must exist in the spermatocytes to control tubule polymerization. This system would need to have two distinct properties: the ability to establish at the appropriate time the correct environment to initiate assembly of the subunits, and some mechanism to order the position of the tubules as they form. It will probably be necessary to investigate both these aspects of the organizing system before we can elucidate the details of the mechanisms by which the spermatids change their shape. Work is now in progress to isolate the tubule material from chicken testis and measure some of the physical and chemical properties of the subunits.

[2] The average tubule in the manchette will be slightly longer than the median nucleus length during this phase. Using the very approximate figure of 13 μ as the length per tubule and 200 as the mean number of tubules per spermatid, we estimate that there are about 2600 μ of manchette tubule. Unpublished pictures of isolated manchette tubules negatively stained with uranyl acetate show that the center-to-center spacing of the subunits along the axis of the tubules is about 50 A. There are, therefore, about 13 subunits for every 50 A of tubule length. The total number of morphological units is thus about $13 \times \frac{2600}{5 \times 10^{-3}} = 6.7 \times 10^6$, on the order of 10^7.

[3] The initial shape of the cytoplasm may be approximated by a hollow spherical shell with an outside diameter of 10 μ and an inside diameter of 6 μ. The volume of such a shell is 410 μ^3. The cytoplasm at the time of manchette formation is approximately a cylindrical shell 22 μ long with an outside diameter of 2 μ and an inside diameter of 1 μ. This shell has a volume of 52 μ^3, about $\frac{1}{8}$ of the initial volume.

APPENDIX

The way in which a helical system of microtubules could give rise to forces which would both constrict the diameter of the nucleus and guide its elongation can be elucidated by looking at several models of helix behavior. Consider first a microtubule of length L wound into a single helix of radius r_o and pitch p (See Fig. *A*). The length of each turn of the helix is $\sqrt{4\pi^2 r_o^2 + p^2}$, which, for $r \gg p$, as in the

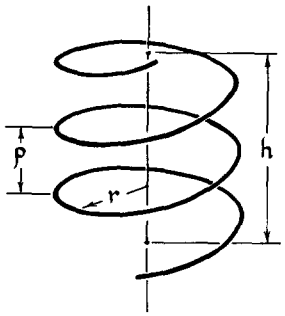

Ⓐ

helix surrounding the spermatid nucleus, is approximately $2\ \pi r_o$. The number of turns in the helix, n_o, is given by

$$n_o = \frac{L}{2\ \pi r_0}, \tag{1}$$

and the axial length of the helix, h_o, is given by

$$h_0 = n_o p. \tag{2}$$

h may be expressed as a function of r by combining (1) and (2) to give

$$h = \frac{pL}{2\ \pi r}. \tag{3}$$

If each turn of the helix is made to slide over the adjacent turn while the pitch is held constant, the arc length per turn of the helix is changed by an amount equal to the slide per turn. Since $2\ \pi r_o$ is the arc length per turn, a decrease in arc requires a decrease in r. If s is the amount of slide for each turn relative to the one below it, then $2\ \pi r_o - 2\ \pi r = s$, or

$$r = r_0 - \frac{s}{2\ \pi}. \tag{4}$$

Using (4) in (3), we find that

$$h = \frac{pL}{2\ \pi r_o - s}. \tag{5}$$

We can now examine the relationship between a single helix and a system of several helices by comparing the helix described above with a set of m intertwined, coaxial helices of the same sense, all lying on the same cylindrical surface. Let each helix have a radius r_o equal to the radius of the single helix and the same axial length h_o; let p be the constant axial spacing separating adjacent helices. Every helix in the set will have a pitch mp. From (2) we see that each one has $\frac{n_o}{m}$ turns and from (1) that the length of each helix must be $\frac{L}{m}$. Note that the total number of turns in the whole system is n_o and the total length of helix is L, just as in the single helix case.

The relation between h and r for each helix in the multiple helix system may be found by substituting the values for pitch and length into (3) to give

$$h = \frac{(mp)\left(\frac{L}{m}\right)}{2\ \pi r} = \frac{pL}{2\ \pi r}. \tag{3'}$$

Since h is the axial length of the whole system and r is the system radius, it is clear from the identity of (3) and (3′) that the same relation governs the dependence of h upon r in either a single or a multiple helix system.

The dependence of r and h on s, however, is altered in the multiple helix case. If there are m helices and s is the slide of one turn over the adjacent turn below, $2\ \pi r_o - 2\ \pi r = ms$ so long as $r \gg mp$. (4) is now modified to give

$$r = r_0 - \frac{ms}{2\ \pi}. \tag{4'}$$

Substituting (4′) into (3′) we find that

$$h = \frac{pL}{2\ \pi r_o - ms} \tag{5'}$$

for a multiple helix system.

We have seen that the dependence of h on r is the same in the two cases, which is to say that, as the turns slide over one another, the shapes of the two systems will change in the same way. However, a comparison of (4) and (5) with their counterparts for the multiple helix system shows that a given amout of sliding of one turn relative to the adjacent one will produce m times as great an effect in the multiple helix system.

A force acting between turns of a helix which acts to move adjacent turns past one another can

thus cause a reduction in helix diameter. If solid material opposes the diameter decrease, a static equilibrium will be established between the outward-directed, radial force in the solid and a tension in the helix (See Fig. *B*). The relation between these quantities can be calculated either by the principle of virtual work or by a force triangle. Both methods show that $T = rF$ where T is the tension in the helix, r is the radius of the helix, and F is the outward force from the solid per unit arc length along the helix. Here again we assume that $r \gg p$.

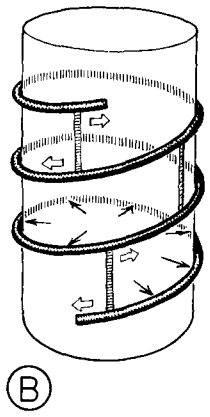

If the material within the helix cannot maintain an outward force of $\frac{T}{r}$ per unit arc length, the helix will constrict in radius and increase in length, imposing a change of shape upon the enclosed space. When the space contains material which is plastic in nature, it will be squeezed out along the axis of the helix where the inward-directed force is absent. We cannot write an expression relating the rate of deformation of the contents to the tension in the helix without knowing both the structural properties of the enclosed material and the physical nature of the mechanism which generates the tension in the helix; this information is not experimentally available at present.

In the helix system surrounding the chicken spermatid nucleus, there are fine connections between adjacent turns, and we have proposed that these cross-bridges generate a force which pushes one turn relative to the next. In this model, any given cross-bridge pushes with an equal force in opposite directions along the arcs of the two helix turns which it connects (See Fig. *B*). All cross-bridges are taken as identical, so the force between every two turns in the system is the same. Evidence from serial sections indicates that there are two helices cross-bridged together, but there is no observable difference between the helices as seen in the electron microscope. We, therefore, propose that they are identical in structure and in their response to cross-bridge action. The effect of the cross-bridges is thus independent of which of the two helices is above and which below the cross-bridge at any given point. Further, from (4′) we see that the presence of two helices doubles the effect of any cross-bridge–induced sliding as compared with the effect which the same amount of slide would produce in a single helix. This advantage may account for the existence of two helices in the chicken spermatid, although it is possible that other factors have also been important, reasons such as an evolutionary pathway or a design consideration in the assembly of the structure.

Part of the work reported here was carried out at the Physiology Department of University College, London; Mr. McIntosh wishes to express his warmest thanks to Professor A. F. Huxley, Dr. and Mrs. Robert Harkness, and Mrs. Lucy Brown for their kind hospitality.

The material presented here will be included in a thesis which will be submitted in partial fulfillment of the requirements for the degree of Doctor of Philosophy at Harvard University.

This work was supported in part by National Institutes of Health grant numbers 5-Fl-GM-23,586 and 5-Tl-GM-707-06.

Received for publication 20 March 1967; revision accepted 8 June 1967.

REFERENCES

1. BEHNKE, O. 1964. A preliminary report on "microtubules" in undifferentiated and differentiated vertebrate cells. *J. Ultrastruct. Res.* **11:** 139.
2. BURGOS, M. H. and D. W. FAWCETT. 1956. An electron microscope study of spermatid differentiation in the toad, *Bufo arenarum* Hensel. *J. Biophys. Biochem. Cytol.* **2:** 223.
3. BYERS, B., and K. R. PORTER. 1964. Oriented microtubules in elongating cells of the developing lens rudiment after induction. *Proc. Natl. Acad. Sci.* **52:** 1091.

4. GIBBONS, I. R. 1963. Studies on the protein components of cilia from *Tetrahymena pyriformis*. *Proc. Natl. Acad. Sci.* **50:** 1002.
5. GRIMSTONE, A. V., and L. R. CLEVELAND. 1965. The fine structure and function of the contractile axostyles of certain flagellates. *J. Cell. Biol.* **24:** 387.
6. GUYER, M. F. 1916. Studies on the chromosomes of the common fowl as seen in testes and in embryos. *Biol. Bull.* **31:** 221.
7. INOUÉ, S. 1959. Motility of cilia and the mechanism of mitosis. *In* Biophysical Science—A Study Program. J. L. Oncley et al., editors. J. Wiley and Sons, New York.
8. KLECZKOWSKI, A. 1963. Protein of tobacco mosaic virus. *Cambridge Phil. Soc. Biol. Rev.* **38:** 364.
9. LAUFFER, M. A., A. T. ANSEVIN, T. E. CARTWRIGHT, and C. C. BRINTON. 1958. Polymerization-depolymerization of tobacco mosaic virus protein. *Nature.* **181:** 1338.
10. LEDBETTER, M. C., and K. R. PORTER. 1964. Morphology of microtubules of plant cells. *Science.* **144:** 872.
11. LUFT, J. H. 1961. Improvements in epoxy resin embedding methods. *J. Biophys. Biochem. Cytol.* **9:** 409.
12. MARKHAM, R., S. FREY, and G. J. HILLS. 1963. Methods for the enhancement of image detail and accentuation of structure in electron microscopy. *Virology.* **20:** 88.
13. MURAYAMA, M. 1966. Molecular mechanism of red cell 'sickling.' *Science.* **153:** 145.
14. NAGANO, T. 1962. Observations on the fine structure of the developing spermatid in the domestic chicken. *J. Cell. Biol.* **14:** 193.
15. PORTER, K. R. 1966. Cytoplasmic microtubules and their functions. *In* Principles of Biomolecular Organization. G. E. W. Wolstenholme and M. O'Connor, editors. J. A. Churchill, Ltd., London.
16. RETZIUS, G. 1909. Biologische Untersuchungen. Vol. XIV, G. Fischer, Jena.
17. REYNOLDS, E. S. 1963. The use of lead citrate at high pH as an electron-opaque stain in electron microscopy. *J. Cell Biol.* **17:** 208.
18. ROBISON, W. G. 1966. Microtubules in relation to the motility of a sperm syncytium in an armored scale insect. *J. Cell Biol.* **29:** 251.
19. SABATINI, D. D., K. BENSCH, and R. J. BARRNETT. 1963. Cytochemistry and electron microscopy: the preservation of cellular ultrastructure and enzymatic activity by aldehyde fixation. *J. Cell Biol.* **17:** 19.
20. TILNEY, L. G. 1965. Microtubules in the asymmetric arms of *Actinosphaerium* and their response to cold, colchicine, and hydrostatic pressure. *Anat. Record.* **151:** 426.
21. TILNEY, L. G., and K. R. PORTER. 1965. Studies on microtubules in Heliozoa—I. *Protoplasma.* **60:** 317.
22. ZLOTNIK, I. 1947. The cytoplasmic components of germ-cells during spermiogenesis in the domestic fowl. *Quart. J. Microscop. Sci.* **88:** 353.